Synthesis and characterization of nano-hydroxyapatite and its application in removal of Fe and Al ions from their aqueous solutions

S. A. Abo-El-Enein[1], H. A. El boraey[2], R. M. El-korashy[3], A. A. Sery[3*]

[1]Chemistry Department, Faculty of Science, Ain Shams University, Egypt
[2]Chemistry Department, Faculty of Science, Menoufia University, Egypt
[3]National Water Research Center, CLEQM, Egypt
chem_alaa.asem@yahoo.com

Abstract: Nano-hydroxyapatite (NHAp) has been synthesized and characterized by means of FTIR, TGA, XRD, TEM and surface area measurements. The resin was applied for the removal of Fe^{2+} and Al^{3+} from their aqueous solutions. Nanomaterials possess novel size-dependent properties because of its high specific surface area, high reactivity, and strong sorption. The uptake values obtained were55.2 and 66.2 mg/g for Fe^{2+} and Al^{3+}, respectively. The data indicated that the adsorption process is endothermic and kinetically follows pseudo-second order model. Langmuir and Freundlich isotherm equations were employed to study the adsorption process. Results indicate that Langmuir isotherm better fits adsorption data than Freundlich model. Factors influencing the removal percent as pH, contact time, adsorbent dose and initial metal ionconcentration have been discussed.
[S. A. Abo-El-Enein, H. A. El boraey, R. M. El-korashy, A. A. Sery. **Synthesis and characterization of nano-hydroxyapatite and its application in removal of Fe and Al ions from their aqueous solutions.** *Nat Sci* 2017;15(3):96-104]. ISSN 1545-0740 (print); ISSN 2375-7167 (online). http://www.sciencepub.net/nature. 14. doi:10.7537/marsnsj150317.14.

Keywords: Nano-hydroxyapatite (NHAp); Nanoparticles; Adsorption; Water treatment.

1. Introduction

Water pollution is the contamination of water bodies (e.g. lakes, rivers, aquifers and groundwater). The contamination of water by heavy metal ions arising from mining operations, textile industries, metal plating, tannery, etc., is a major environmental problem. The release of large quantities of heavy metal ions into the natural environment e.g. irrigation of agricultural fields by using sewage has resulted in a number of environmental problems [1]and due to their non-biodegradability and persistence, can accumulate in the environment elements such as food chain, and thus may pose a significant danger to human health[2]. Many methods that are being used for removal of heavy metal ions include chemical precipitation, filtration, evaporation, electrolysis, cementation, reverse osmosis, Ultraviolet light [3], Boiling and Low frequency ultrasonic irradiation [4]. Adsorption process appears to be the most effective, especially for effluents with moderate and low concentrations. It has received more attention and largely application due to many factors: simplicity of design, high efficiency with high uptake capacity and low cost during the multi-adsorption interaction processes[5].

In the area of water purification, nanotechnology gives the possibility of an efficient removal of pollutants. Nanotechnology is the engineering of manipulating matter at the nanoscale (1-100 nm) [6]. At this scale, materials possess novel size-dependent properties which are different from their large counterparts because of its high specific surface area, high reactivity, and strong sorption. Others take advantage of their discontinuous properties, such as super para-magnetism and quantum confinement effect. Hydroxyapatite (HAp) is one of the most popular phosphates, with a chemical formula $Ca_{10}(PO_4)_6(OH)_2$. The common crystal phase is hexagonal, but the monoclinic phase can be present[7]. Up to 50% by volume and 70% by weight of human bone is a modified form of hydroxyapatite (known as bone mineral). HAp can be synthesized in the laboratory by many methods including the sol-gel process [8], hydrothermal synthesis [9], microwave synthesis [10], ultrasonic spray pyrolysis [11], wet precipitation [12], emulsion system synthesis and sonochemical synthesis[13].

The specific properties of NHAp are related to various surface characteristics, e.g., surface functional groups, acidity and basicity, surface charge, hydrophilicity and porosity. HAp has been used for the removal of many pollutants from contaminated soils and wastewater [14, 15]. HA was used in removal of lead ions [16]. The optimum dose of HA for Pb (II) removal is found to be 0.12 g/L with the removal efficiency of 97.3 %. It is found that the adsorption kinetics of the Pb (II) on HA follow the pseudo second-order reaction. Langmuir isotherm had best fit than Freundlich, Halsey, and Harkins–Jura isotherms for experimental data.

The ability of nano-hydroxyapatite (nano-HAP) to adsorb aqueous Cd, Pb and Cu ions from single-

metal and multi-metal ions reaction systems had been tested [17]. For mono-metal reaction systems, results showed that the sorption of metals on nano-HAP are well fitted both using the Langmuir and Freundlich equations. The hydroxyapatite was used as an alternative low-cost adsorbent material to study the adsorption behavior of La (III) and Eu (III) ions from nitrate aqueous solutions.

The objective of this study is to investigate the removal efficiency of nano-hydroxyapatite (NHAp) as an alternative adsorbent for the removal of Fe^{2+} and Al^{3+} cations from aqueous solutions.

2. Experimental

2.1. Chemicals

Di-ammonium hydrogen-phosphate, $(NH_4)_2HPO_4$, Calcium nitrate tetrahydrate, $Ca(NO_3)_2.4H_2O$ and ammonia solution, NH_4OH, were used for the synthesis of NHAp powder. Ammonium iron (II) sulfate, or Mohr's Salt, $(NH_4)_2Fe(SO_4)_2 \cdot 6H_2O$ and Potassium aluminum sulfate dodecahydrate, $KAl(SO_4)_2 \cdot 12H_2O$ were used as sources of Fe^{2+} and Al^{3+}, respectively. All chemicals were purchased from Sigma-Aldrich Company and used without further purification.

2.2. Synthesis of HApnanopowder particles:

Nano-HAp, $Ca_{10}(PO_4)_6(OH)_2$, was synthesized via solution-precipitation method [18]. In this method $(NH_4)_2HPO_4$ and $Ca(NO_3)_2.4H_2O$ are used as starting materials and ammonia solution for pH adjustment. A suspension of 116.05 gm of $Ca(NO_3)_2.4H_2O$ was vigorously stirred at constant temperature 25ºC. A solution of 39.6 gm of $(NH_4)_2HPO_4$ was slowly added dropwise to the suspended $Ca(NO_3)_2.4H_2O$. The pH was kept 11 in all experiments using ammonia suspended solution. This can be explained by the following reaction:

$$10\ Ca(NO_3)_2.4H_2O + 6\ (NH_4)_2HPO_4 + 8\ NH_4OH$$
$$Ca_{10}(PO_4)_6(OH)_2 + 20\ NH_4NO_3 + 20\ H_2O$$

In The next step nano-HAp resin was precipitated and removed from the solution by centrifugation at speed of 3000 rpm. The precipitate was dried at 100 ºC.

2.2. Characterization of NHAp adsorbent:

The FT-IR spectra of the NHAp adsorbent were recorded on a Pye-Unicam Sp-883 Perkins-Elmer spectrophotometer between 4000 and 400 cm^{-1}. Thermogravimetric analysis was carried out in a nitrogen atmosphere using Shimadzu DT/TG-50. The flow rate of N_2 was adjusted at 20 mL/min. The specific surface area and average pore diameter were measured by a Quanta chrome NOVA system using nitrogen gas as adsorbate at liquid nitrogen temperature (77 K). The nanostructure of NHAp powder was studied using high resolution transmission electron microscopy (HRTEM). The nanopowders were analyzed by X-ray diffraction (XRD) with Siemens-Brucker D5000 diffractometer using Cu-Kα radiation (1.540600 Å). For qualitative analysis, XRD patterns were recorded in the range of $10º \leq 2\theta \leq 80º$.

2.4. Preparation of solutions:

Stock solutions of Fe(II) and Al (III) with concentration of 1000 ppm were prepared by dissolving the weights of ammonium iron(II) sulfate and potassium aluminum sulfate dodecahydratein distilled water. Fresh dilutions were used in each experiment.

2.5. Uptake experiments:

2.5.1. Effect of initial metal ion concentration

The effect of initial metal ion concentration on the removal percent was determined at fixed adsorbent dose (1 g/L), time of 120 min and temperature (25°C) with different metal ion concentrations 10-250 ppm in 50 ml solution shaked at 135 rpm. The removal percent of heavy metal ions was calculated by determining the residual concentration of each metal ion through Inductively Coupled Plasma (ICP), Optima 5300 DV- Perkin-Elmer. The removal percent of heavy metal ions was calculated using the following equation:

$$\%\ \mathbf{Removal} = \frac{(C_0 - C_e)}{C_0} \times 100 \quad (1)$$

where, C_0 is the initial concentration of metal ion (ppm);

C_e is the equilibrium metal ion concentration after adsorption (ppm).

The adsorption capacity, q_e (mg metal per g adsorbent) can be calculated from the equation:

$$q_e = (C_0 - C_e)\frac{V}{w} \quad (2)$$

where, V (Liter) is the solution volume and w (Gram) the amount of adsorbent.

2.5.2. Effect of initial pH

Adsorption of Fe^{2+} and Al^{3+} on NHAp adsorbents under controlled pH was carried out using 0.05 g of dry adsorbent in a series of flasks contains 50 mL of a specific metal ion solution of concentration 100and 60 ppm for Fe and Al, respectively. The pH was adjusted using HCl and NaOH. The flasks were conditioned on a vibromatic shaker and 25 ±1ºC with equilibration time of 60 min. The pH of the working solutions were measured using a pH-meter.

2.5.3. Effect of contact time

The effect of contact time on the uptake of Fe^{2+} and Al^{3+} on NHAp adsorbent was investigated using 0.05 g of adsorbent in a series of flasks each containing 50 mL of a specific metal ion solution and the natural pH of metal ion solutions. The samples were taken at predetermined time intervals ranging from 5 to 120 min. The residual concentration of the metal ion was determined.

2.5.4. Effect of ionic strength

Different values of Potassium chloride KCl(0.1-0.5 g/50 mL, 0.05 g adsorbent) were added to metal ions solutions with affixed concentration of metal ion. After 60 min of continuous shaking, the solutions were centrifuged and then filtered.

2.5.5. Effect of dosage

Experiments were carried out taking different amounts of nano-adsorbent (0.025-0.1 g /50mL) keeping the heavy metal ion parameters constant.

3. Results and discussion

3.1. Characterization of nanomagnetic-hydroxyapatite adsorbent

The FTIR spectrum of NHAp powder was scanned in the range of 4000-400 cm^{-1}. IR spectra indicate that spectra possess broad bands near 3500-3300 and 1629 cm^{-1} due to strongly adsorbed and bound water in the adsorbent materials. A strong band appears at 3141cm^{-1} for NHAp which is due to the vibrational of hydroxyl ions; the peak appeared at 1030 cm^{-1} is attributed to stretching vibrations of PO_4^{3-} while the bands located at (1385, 602 and 563 cm^{-1}) are corresponding to the bending vibrations of PO_4^{3-}. The results obtained are shown in **Fig. 1** and given in **Table 1**.

The XRD pattern of NHAp powders is shown in **Fig. 2**. Several diffraction peaks are observed at 2θ= 22.4, 26.3, 28.87, 30.15, 32.8 and 40.9 which are characteristic for NHAp. The sharp intensities of the diffraction peaks confirmed the well crystalline nature of NHAp.

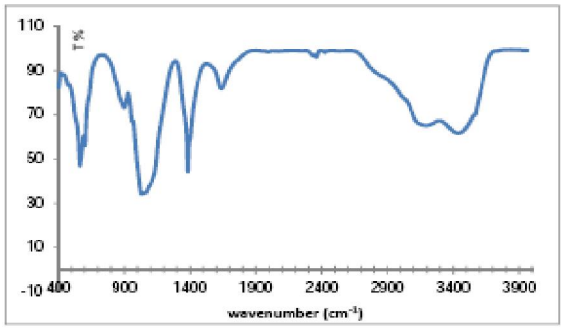

Fig. 1. FTIR spectra of Nano-hydroxyapatite

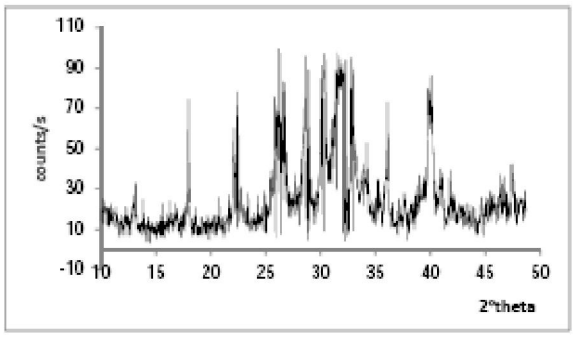

Fig. 2: XRD pattern of nano-HAp adsorbent

Table 1: Assignments of observed vibrational frequencies of NHAp powder.

Assignments	**NHAp**
Structural OH^-	3141.1
H_2O absorbed	1627.9
CO_3^-	894.9
PO_4^{3-} bend ν_3	1385.7
PO_4^{3-} stretch ν_1	1030.0
PO_4^{3-} bend ν_4	602.2
PO_4^{3-} bend ν_4	563.8

The BET surface area and pore properties are determined by observing adsorption–desorption behavior of nitrogen on the adsorbent. This behavior gives information about the pore size that is accessible and can be occupied by pollutants. From **Table 2**, the recorded mean hydraulic radii are in the range of 4.5-10 nm revealing the mesoporous nature of the prepared solid. The specific surface area of the prepared sample is about 31.02 m^2/g.

Table 2: NHAp adsorbent properties

	NHAp
Mean pore diameter	10.0 nm
Total pore volum (p/p_0 =0.903)	8.22 cm^3g^{-1}
Surface area	31.02 m^2/g

The morphology and nanostructure of NHA padsorbentare studied using high-resolution transmission electron microscopy (HRTEM). The TEM micrograph obtained for NHAp displays the predominance of thin needle-like particles having lengths ranging from 21.9 to 44.04 nm with cross-sectional sizes ranging from 7.15 to7.83 nm, **Fig. (3)**.

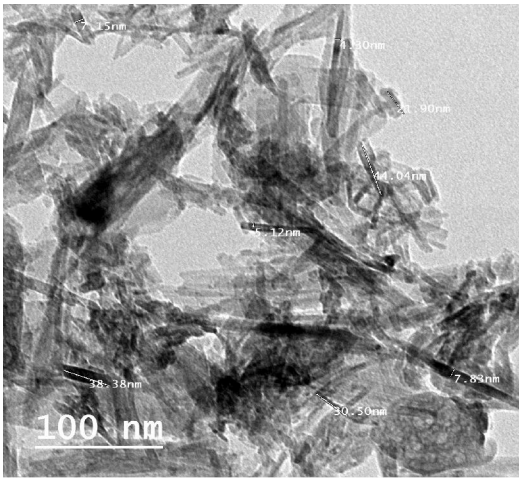

Fig. 3. HRTEM micrographs of NHAp adsorbent

TGA curve for pure composite (Fig. 4) shows an initial weight loss of about 6.26% between ambient temperature and 100℃ which attributed to evolution of

physical adsorbed water followed by second stage of weight loss by about 34% due to dehydroxylation of the composite. Finally, a weight loss by about 6% between 400 and 600℃ is attributed to decomposition of phosphate.

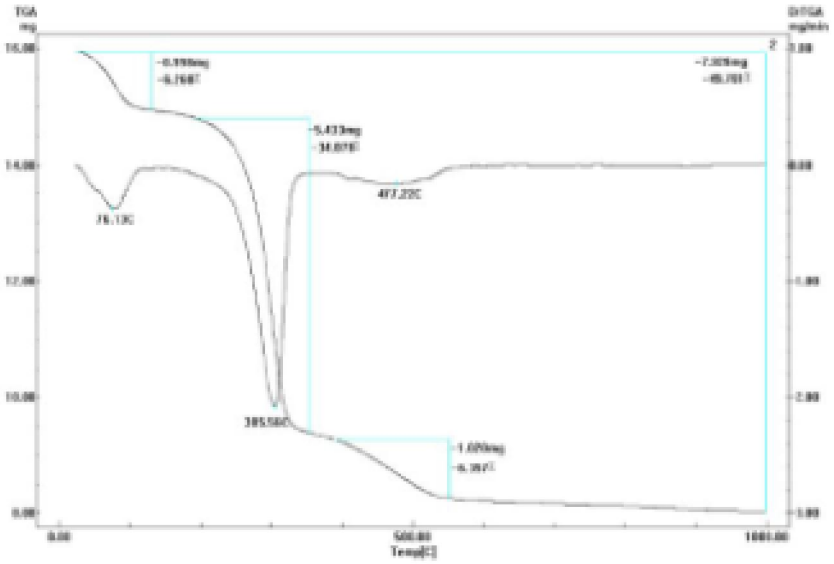

Fig. 4. Thermograme of NHAp adsorbent.

3.2. Adsorption studies

Factors influencing the removal heavy metal ions removal from their aqueous solutions were investigated to properly choose the optimizing parameters of the adsorption process.

3.2.1. Effect of initial metal ion concentration on metal ion uptake

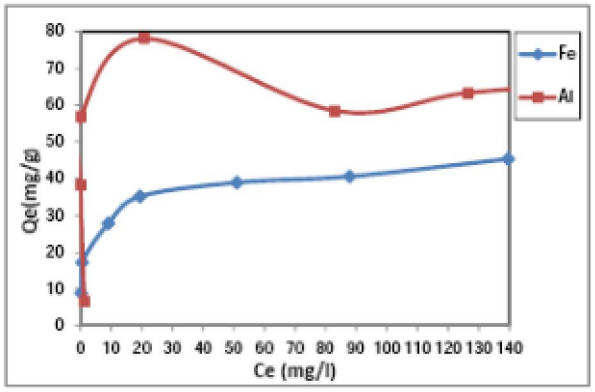

Fig. 5. Effect of initial metal ion concentration on the uptake of Fe (II) and Al (III) using NHAp as adsorbent at 25ºC.

The metal ions adsorption mechanism is particularly dependent on the initial metal ions concentration; at low concentrations, metals are adsorbed by specific active sites. With increasing metal ion concentrations the sorption sites are saturated[19].. **Fig. 5**shows the plot of experimental data for the adsorption of different metal ions on NHAp as a function of equilibrium concentration(C_e) of metal ion at different initial metal ion concentrations. As shown, the q_e-values increase with increasing initial metal ion concentration. The maximum q_e-values obtained for Fe (II) and Al(III) on nano-hydroxyapatite are 55.2, 66.2 mg/g, respectively. These results confirmed that the initial metal ions concentration played an important role in the adsorption process on NHAP surface. The adsorption capacity decreases in the following order Al (III) > Fe (II).

3.2.2. Effect of pH on metal ion uptake

Hydrogen ion concentration is an essential parameter in the adsorption study which affect the adsorption behavior of heavy metal ions in aqueous solutions. Adsorption of different metal ions on the adsorbent materials under consideration was studied at varying pH values to optimize the maximum metal ion removal. NHAp has hydroxyl groups (OH^-) which carry negative charges that allow the adsorbent to be potential binding sites for cations[20]. The removal of Al (III) increases from27.1% at pH 2 to 99% at pH 7. The relationship between pH and metal ion removal is shown in **Fig. 6**. Since high proton concentration at lower pH, heavy metal ion uptake was decreased due to the positive charge density on metal ion binding sites. The negative charge density on the cell surface increases with increasing in pH due to de-protonation

of binding sites. The metal ions then become more competitive against to bind the sites which increases the metal ion uptake[21]. Studies at pH 4 for iron were not attempted because precipitation of the ions as hydroxides is expected[22].

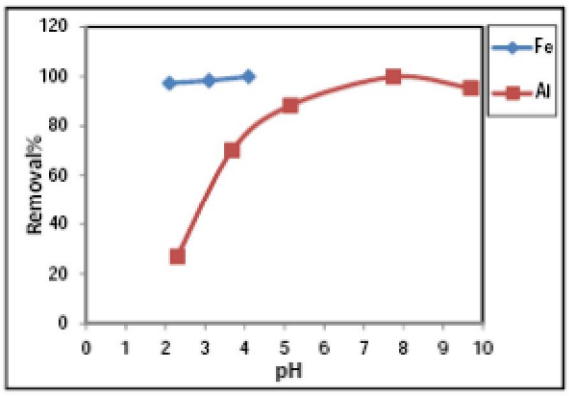

Fig. 6. Effect of pH on the removal percent of Fe (II) and Al (III)) on NHAp at 25ºC.

3.2.3. Effect of contact time on metal ion uptake

Equilibrium time is an important parameter for an economical wastewater treatment system. In general for a given concentration, the amount of metal ion adsorbed increases rapidly with time at the beginning, then non-linearly at a slower rate and finally attain saturation at equilibrium time, which is dependent on concentration for each adsorbent. Basically, the rapid increase in sorption is because initially the adsorption sites are more available and the metal ions are easily adsorbed on these sites.

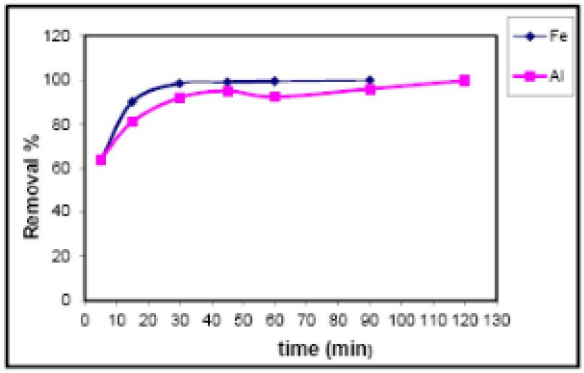

Fig. 7. Effect of contact time on the removal percent of Fe (II) and Al (III) on NHAp at 25ºC.

The results of adsorption of metal ions on NHAp as function of time are shown in **Fig. 7**. The percent metal ions removal increased rapidly for Fe(II) and Al(III) in the beginning due to the presence of a larger number of active adsorption sites on the surface of adsorbent being available for the adsorption of the metal ions. Evidently, the equilibrium time for these metal ions is regarded to be about 60 min. for further applications.

3.2.4. Effect of adsorbent dosage on metal ion uptake

It is evident that the efficiency increases for all of the heavy metal ions. The increase in the efficiency is due to an increase in the number of active sites on the surface of the different nanoparticles available for the reaction, which in turn increases the rate of adsorption [23]. The removal efficiency of iron ions increases from 77.9 % to 99.4% when NHAp dose increases from 0.025 to 0.1 g /50 mL at the end of 60 min (**Fig. 8).** In case of aluminum ions the removal percent increases from 83.2 % to 99.3% after 60 min when the adsorbent dose increases from 0.025 to 0.1 g/50 mL.

3.2.5. Effect of salinity on metal ion uptake

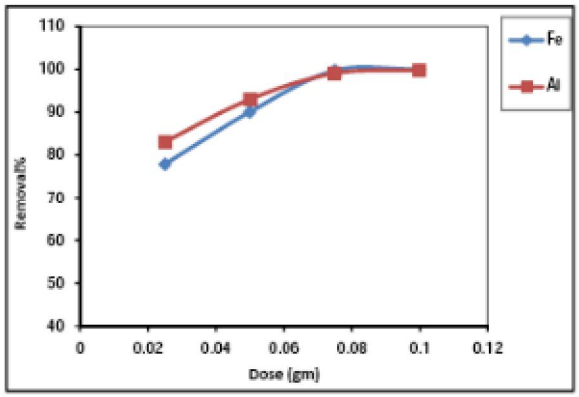

Fig. 8. Effect of adsorbent dosage on the removal percent of Fe (II) and Al (III) on NHAp at 25ºC.

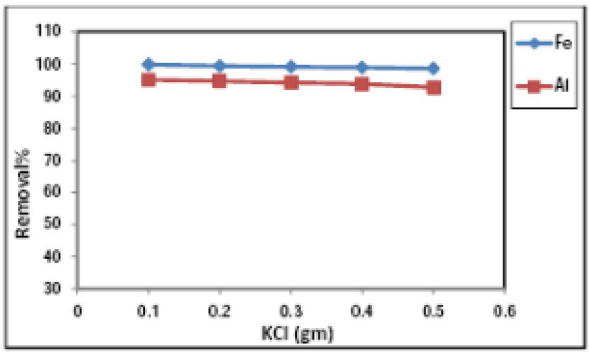

Fig. 9. Effect of salinity on the removal percent of Fe (II) and Al (III) on NHAp at 25ºC.

The Influence of salinity on heavy metal ions sorption was investigated to determine solution chemistry effects. The effect may be different for different metal ions and adsorbents. Generally, adsorption decreases with increasing ionic strength of the aqueous solution[24]. The electrostatic attraction at low ionic strength appears to play a negligible role

in the removal of metal ions for sorbent. The results for NHAp as adsorbent indicate that there was a slight decrease in the removal of Fe(II) and Al (II) ions for the interval of salinity studied. Therefore, this adsorbent can be applied for heavy metal ions removal from wastewaters containing high amount of salts. The data obtained are shown in **Fig. 9**.

3.2.6. Adsorption isotherms

3.2.6.1. Langmuir's model

The Langmuir adsorption isotherm has been applied successfully to many pollutants adsorption processes and has been the most widely used sorption isotherm for the sorption of a solute from a liquid solution assuming that all sites of adsorption have the same energy[25]. The saturated monolayer isotherm can be represented as follows:

$$\mathbf{q_e = \frac{Q_0 k C_e}{1+kC_e}} \ldots\ldots\ldots\ldots \quad (3)$$

This equation can be rearranged to the common linear form:

$$\frac{C_e}{q_e} = \frac{1}{Q_0 k} + \frac{C_e}{Q_0} \ldots\ldots\ldots\ldots \quad (4)$$

Where C_e is the equilibrium concentration (mg/L); q_e is the amount of metal ion adsorbed per unit mass of adsorbent (mg/g); Q_0 is q_e for a complete monolayer (mg/g), and k is a constant related to the affinity of the binding sites and energy of adsorption (L/mg). K represents enthalpy of sorption and should vary with temperature. A high K value implies a high affinity. The values of Q_0 and k for this adsorbent are determined, respectively, from slopes and intercepts of the linear plots of C_e/q_e vs. C_e.

The adsorption parameters for the adsorption of Fe(II) and Al(III) on NHAp adsorbent are collected in **Table 3**. The plot of C_e/q_e vs. C_e as shown in **Fig.(10),** gives a straight line with slope and intercept of $1/Q_0$ and $1/K\ Q_0$, respectively. This indicates that the adsorption process is limited to monolayer formation and proceeds according to Langmuir's isotherm. At the same temperature, the binding constant (K) follows the order $Al^{3+} > Fe^{2+}$. This is related to the nature and the strength of interaction. The higher the values of R^2, the more applicable the model for the metal ion examined. According to the value of Q_0 parameter, the sorption of metal ions on NHAp can follow the sequence $Al^{3+} > Fe^{2+}$. The preference of sorption exhibited by the nano-hydroxyapatite for Al^{3+} over Fe^{2+} may be attributed to Al's smaller hydrated radius (Al^{3+}= 0.053 nm and Fe^{2+} = 0.077 nm) and hydration energy (Al^{3+} = -4659.7 kJ/mol, Fe^{2+} = -1950 kJ/mol)[104]. Another reason may explain the sequence; the groups present on the nano-hydroxyapatite are OH^- and PO_4^{-3} group, which are hard Lewis bases. Al^{3+} is a hard Lewis acid while Fe^{2+} is a borderline intermediate Lewis acid. This could be one of the reasons for greater affinity of Al^{3+} as compared to Fe^{2+}.

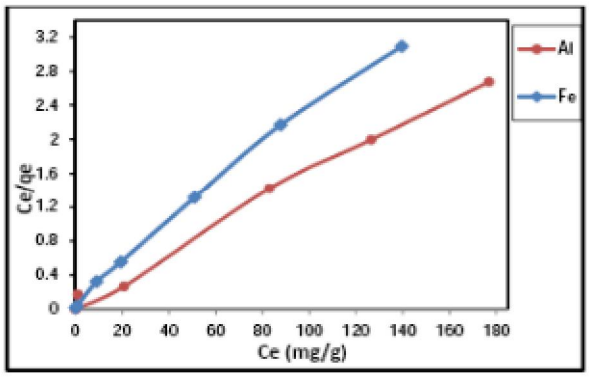

Fig. 10. Langmiur adsorption isotherms of Fe (II) and Al (III) on NHAp at 25ºC.

3.2.6.2. The Freundlich model

Meanwhile, the Freundlich isothermassumes that the adsorption occurs on heterogeneous surface at sites with different energies of adsorption (heteroenergytic surface)[26]. Mathematically this model is characterized by the heterogeneity factor (1/n). Freundlich model can be represented by the linear form as follows:

$$\ln q_e = \ln K_F + \frac{1}{n} \ln C_e \ldots\ldots\ldots\ldots \quad (5)$$

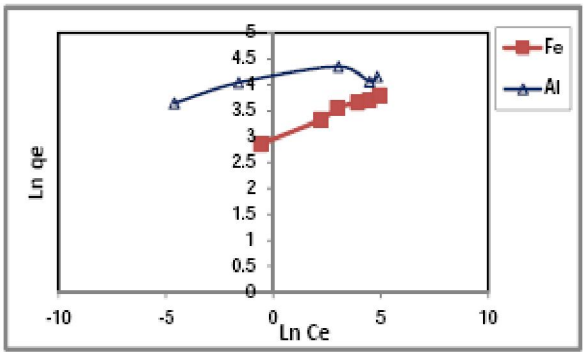

Fig. 11. Freundlish adsorption isotherms of Fe (II) and Al (III) on NHAp at 25ºC.

where, K_F is the Freundlich constant (mg/g)/ (L/mg) and n is the heterogeneity factor. While 1/n value is related to the adsorption intensity. When 1/n values are in the range $0.1 < 1/n < 1$, the adsorption process is favorable [27]**.** A plot of $\ln q_e$ versus $\ln C_e$, gives a straight line and the values of K_F and 1/n can be determined from the intercept and the slope, respectively. If n is below one, the adsorption is chemical process; otherwise, the adsorption is a physical process [28]. All values of n exceed one, indicating that the adsorption is physical process as indicated from the results were given in **Table 3** and shown graphically in **Fig. 11**.

However, the coefficient R^2 values exceed 0.9 for Langmiur model while they are low for all heavy metal ions in Feundlich model suggesting that the Langmuir model is fitted with the experimental results obtained.

Table 3: Isothermic parameters of NHAp adsorbent

	Langmiur isotherm			**Freundlich isotherm**			
Metal	Q_o	K	R^2	1/n	n	K_f	R^2
Fe	44.84	0.24	0.99	0.172	5.81	19.4	0.98
Al	65.78	0.327	0.99	0.0485	20.6	53.9	0.60

3.2.7. Adsorption kinetic study

The adsorption/time data obtained were applied on two kinetic models, namely the pseudo-second-order and pseudo-first-order models.

3.2.7.1. Pseudo-first-order model.

The pseudo-first-order model is expressed as:

$$\log (q_e - q_t) = \log q_e - \left(\frac{k_1}{2.303}\right) t \quad (6)$$

where, q_e and q_t represent the values of amount adsorbed at time (t) and at equilibrium, respectively and k_1 is the rate constant of pseudo-first order (min^{-1}). These parameters are determined from the linear plots of log ($q_e - q_t$) vs. (t) shown in **Fig. 12**. The validity of the model is checked by the fitness of the factor (R^2). From their intercept and slope, the values K_1 and q_e are calculated.

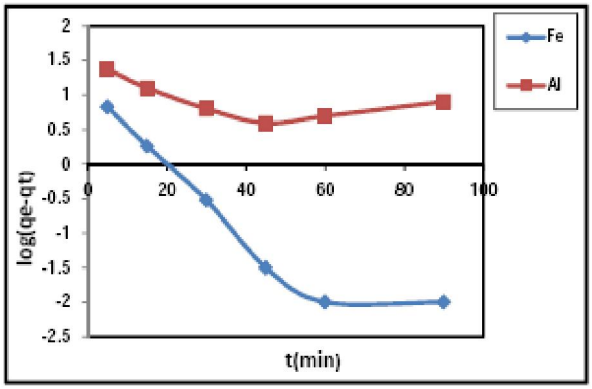

Fig. 12. Pseudo-first order kinetic model of the uptake of Fe (II) and Al (III) on NHAp.

3.2.7.2. Pseudo-second-order model

The pseudo-second-order model is expressed as[29]:

$$\frac{t}{q_t} = \frac{1}{k_2 q_e^2} + \frac{1}{q_e} t \quad \ldots\ldots\ldots\ldots\ldots (7)$$

where, k_2 is the pseudo-second order rate constant of adsorption (g. mg^{-1}. min^{-1}), q_e and q_t (mg/g) are the amount of metal ions adsorbed at equilibrium and at time (t), respectively. The different kineticparameters for the adsorption of Fe^{2+} and Al^{3+} on NHAp surface are cited in **Table 4**. The plot of t/q_t vs. t gave straight lines for the two heavy metal ions as shown in **Fig. 13**. The validity of each model was checked by the fitness of the straight line (R^2). The results indicate that the R^2values obtained for the pseudo-second order are higher than those obtained for the first-order kinetic model; this implies that the pseudo-second order model fitted with the results obtained.

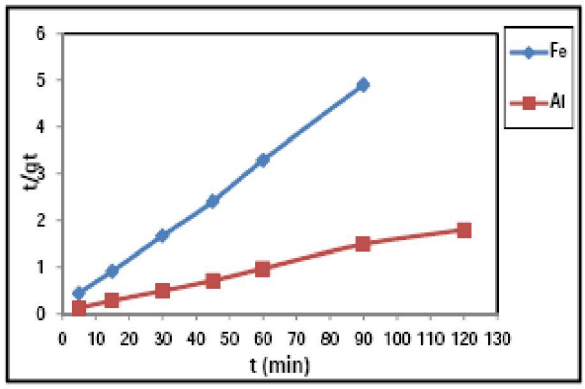

Fig. 13. Pseudo-second order kinetic model of the uptake of Fe (II) and Al(III) on NHAp.

Table 4: Adsorption Kinetic parameters for different kinetic models of NHAp.

	Pseudo-second order			**Pseudo-first order**		
Metal ion	**K_2 ($gmg^{-1}min^{-1}$)**	**q_e (mg/g)**	**R^2**	**K_1 $(min)^{-1}$**	**q_e (mg/g)**	**R^2**
Fe	0.0252	18.97	0.99	0.0819	4.28	0.85
Al	0.0053	66.22	0.99	0.012	13.43	0.34

3.2.8. Adsorption Thermodynamics:

Thermodynamic parameters such as enthalpy change (ΔH°), free energy change (ΔG°) and entropy change (ΔS°) must be taken into consideration in order to determine the spontaneity of a process. The thermodynamic parameters were obtained from adsorption experiments at several temperatures (298, 308, 318 and 328 K) and were estimated using equations [9-11], [30]:

$$K_c = C_{ad} / C_e \ldots\ldots\ldots\ldots\ldots\ldots \quad (9)$$

$$\ln K_c = \Delta S^\circ / R - \Delta H^\circ / RT \ldots\ldots\ldots\ldots \quad (10)$$

$$\Delta G^\circ = -RT \ln K_c \ldots\ldots\ldots\ldots\ldots \quad (11)$$

where, K_c is the equilibrium constant, C_{ad} (mg/L) is the metal ion concentration adsorbed on the solid surface at equilibrium, C_e (mg/L) is the equilibrium concentration of metal ion in the solution, R (8.314 J/(K.mol)) is the universal gas constant and T is absolute temperature. The values of ΔH° and ΔS° were obtained from the slope and intercept of Van't Hoff equation and a plot of $\ln K_c$ versus 1/T(**Fig. 15**). The data given in **Table 5** shows that $|\Delta H^\circ| < |T\Delta S^\circ|$ at all temperatures. This indicates that the adsorption process is dominated by entropic rather than enthalpic changes. The results obtained of ΔG° are -8.671 kJ mol^{-1} at 25 °C and -6.367 kJ mol^{-1}, for Fe and Al ions, respectively. These ΔG°-values indicate that the adsorption is physisorption and spontaneous process. Apparently, the positive enthalpy change values indicate the endothermic nature of the process at the temperatures under study. The observed increase in ΔG° value with temperature indicates that the adsorption process is more favorable at higher temperatures. Moreover, the positive entropy ΔS° values implied that the degree of randomness increase at solid-liquid interface.

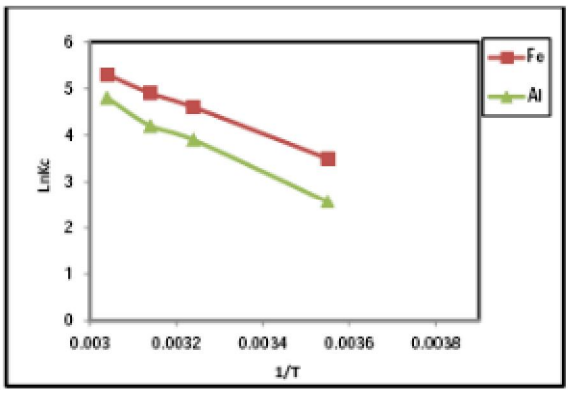

Fig. 14. Plot of ln K_C vs. 1/T for estimation of thermodynamic parameters for the adsorption of Fe (II) and Al (III) on NHAp.

Table 5: Thermodynamic parameters of NHAp adsorbent.

Metal ion	T^o k	K_c	r^2	ΔG°(KJmol^{-1})	ΔS° (KJmol^{-1})	ΔH° (KJmol^{-1})
Fe	298	34.1	0.999	-8.671	0.12329	29.069
	308	104.5		-11.77		
	318	141.3		-12.95		
	328	206		-14.45		
Al	298	13.16	0.993	-6.367	0.1469	35.400
	308	52.02		-9.986		
	318	72.9		-11.104		
	328	126		-13.089		

4. Conclusion

In this study, nano-hydroxyapatite was synthesized and characterized. The prepared sample was confirmed as an effective adsorbent for the removal of Fe (II) and Al (III) ions from aqueous solutions. The specific surface area of the prepared sample is about 31 m^2/g, nanostructure of needle-like particles and with a mesoporous nature. The maximum equilibrium q_e-values obtained for Fe (II) and Al(III) on NHAp are 55.2, 66.2 mg/g, respectively. The thermodynamic data also reveal that the adsorption process is dominated by entropy changes as $|\Delta H^\circ| < |T\Delta S^\circ|$ at all temperatures. The pseudo-second order model is fitted with the results obtained. Langmiur isotherm better fits adsorption data rather than the Freundlich model. These characteristics make NHAp adsorbent a good nominate in the field of wastewater treatment.

References

1. Kaewsarn, P. and Yu, Q., Cadmium (Ii) Removal from Aqueous Solutions by Pre-Treated Biomass of Marine Alga Padina Sp, Environmental pollution. 112**:** (2) (2001) 209-213.
2. Zhou, Q., et al., Biomonitoring: An Appealing Tool for Assessment of Metal Pollution in the Aquatic Ecosystem, Analytica chimica acta. 606**:** (2) (2008) 135-150.
3. Droste, R., *Theory and Practice of Water and Wastewater Management Systems*, 1997, Wiley, New York, NY.
4. Gupta, S. K., Behari, J., and Kesari, K. K., Low Frequencies Ultrasonic Treatment of Sludge, Asian Journal of Water, Environment and Pollution. 3**:** (2) (2006) 101-105.

5. Zhao, X., et al., Adsorption Investigation of Ma-Dtpa Chelating Resin for Ni (Ii) and Cu (Ii) Using Experimental and Dft Methods, Journal of Molecular Structure. 986**:** (1) (2011) 68-74.
6. Sample, J. L. and Charles Jr, H. K., Systems Engineering at the Nanoscale, Johns Hopkins APL Technical Digest. 31**:** (1) (2012) 50-57.
7. Marasaraju, T. and Phebe, D., Some Physicochemical Aspects of Hydroxyapatite, J. Mater. Sci. 31**:** (1) (1996) 1-21.
8. Andersson, J., et al., Sol–Gel Synthesis of a Multifunctional, Hierarchically Porous Silica/Apatite Composite, Biomaterials. 26**:** (34) (2005) 6827-6835.
9. Wang, Y., et al., Hydrothermal Synthesis of Hydroxyapatite Nanopowders Using Cationic Surfactant as a Template, Materials Letters. 60**:** (12) (2006) 1484-1487.
10. Liu, J., et al., Rapid Formation of Hydroxyapatite Nanostructures by Microwave Irradiation, Chemical physics letters. 396**:** (4) (2004) 429-432.
11. Aizawa, M., et al., Characterization of Hydroxyapatite Powders Prepared by Ultrasonic Spray-Pyrolysis Technique, Journal of materials science. 34**:** (12) (1999) 2865-2873.
12. Silva, C. C., et al., Hydroxyapatite Screen-Printed Thick Films: Optical and Electrical Properties, Materials Chemistry and Physics. 92**:** (1) (2005) 260-268.
13. Kim, W. and Saito, F., Sonochemical Synthesis of Hydroxyapatite from H 3 Po 4 Solution with Ca (Oh) 2, Ultrasonics Sonochemistry. 8**:** (2) (2001) 85-88.
14. Barka, N., et al., Removal of Reactive Yellow 84 from Aqueous Solutions by Adsorption onto Hydroxyapatite, Journal of Saudi Chemical Society. 15**:** (3) (2011) 263-267.
15. Mourabet, M., et al., Removal of Fluoride from Aqueous Solution by Adsorption on Hydroxyapatite (Hap) Using Response Surface Methodology, Journal of Saudi Chemical Society. 19**:** (6) (2015) 603-615.
16. Ramesh, S., et al., Adsorptive Removal of Pb (Ii) from Aqueous Solution Using Nano-Sized Hydroxyapatite, Applied Water Science. 3**:** (1) (2013) 105-113.
17. Chen, S., et al., Adsorption of Aqueous Cd2+, Pb2+, Cu2+ Ions by Nano-Hydroxyapatite: Single- and Multi-Metal Competitive Adsorption Study, Geochemical journal. 44**:** (3) (2010) 233-239.
18. Valsami-Jones, E., et al., The Dissolution of Apatite in the Presence of Aqueous Metal Cations at Ph 2–7, Chemical Geology. 151**:** (1) (1998) 215-233.
19. Aksu, Z., Application of Biosorption for the Removal of Organic Pollutants: A Review, Process Biochemistry. 40**:** (3) (2005) 997-1026.
20. Yin, P., et al., Biosorption Removal of Cadmium from Aqueous Solution by Using Pretreated Fungal Biomass Cultured from Starch Wastewater, Water Research. 33**:** (8) (1999) 1960-1963.
21. Kapoor, A., Viraraghavan, T., and Cullimore, D. R., Removal of Heavy Metals Using the Fungus Aspergillus Niger, Bioresource technology. 70**:** (1) (1999) 95-104.
22. Morgan, B. and Lahav, O., The Effect of Ph on the Kinetics of Spontaneous Fe (Ii) Oxidation by O 2 in Aqueous Solution–Basic Principles and a Simple Heuristic Description, Chemosphere. 68**:** (11) (2007) 2080-2084.
23. Gupta, V. K., et al., Photo-Catalytic Degradation of Toxic Dye Amaranth on Tio 2/Uv in Aqueous Suspensions, Materials Science and Engineering: C. 32**:** (1) (2012) 12-17.
24. Baker, H. M., Massadeh, A. M., and Younes, H. A., Natural Jordanian Zeolite: Removal of Heavy Metal Ions from Water Samples Using Column and Batch Methods, Environmental monitoring and assessment. 157**:** (1-4) (2009) 319-330.
25. Langmuir, I., The Constitution and Fundamental Properties of Solids and Liquids. Part I. Solids, Journal of the American Chemical Society. 38**:** (11) (1916) 2221-2295.
26. Walker, G. and Weatherley, L., Adsorption of Dyes from Aqueous Solution—the Effect of Adsorbent Pore Size Distribution and Dye Aggregation, Chemical Engineering Journal. 83**:** (3) (2001) 201-206.
27. Vázquez, I., et al., Removal of Residual Phenols from Coke Wastewater by Adsorption, Journal of Hazardous Materials. 147**:** (1) (2007) 395-400.
28. Jiang, J.-Q., Cooper, C., and Ouki, S., Comparison of Modified Montmorillonite Adsorbents: Part I: Preparation, Characterization and Phenol Adsorption, Chemosphere. 47**:** (7) (2002) 711-716.
29. Guibal, E., Milot, C., and Tobin, J. M., Metal-Anion Sorption by Chitosan Beads: Equilibrium and Kinetic Studies, Industrial & Engineering Chemistry Research. 37**:** (4) (1998) 1454-1463.
30. Kamari, A. and Ngah, W. W., Isotherm, Kinetic and Thermodynamic Studies of Lead and Copper Uptake by H 2 So 4 Modified Chitosan, Colloids and Surfaces B: Biointerfaces. 73**:** (2) (2009) 257-266.

2/19/2017